Calculation of force distribution for a periodically supported beam subjected to moving loads

Tien Hoang, Denis Duhamel, Gilles Forêt, Honoré P. Yin, P. Joyez, R. Caby

Calculation of force distribution for a periodically supported beam subjected to moving loads

T. Hoang[a,*], D. Duhamel[a], G. Foret[a], H.P. Yin[a], P. Joyez[b], R. Caby[b]

[a] *Université Paris-Est, Navier (UMR 8205 ENPC-IFSTTAR-CNRS), Ecole Nationale des Ponts et Chaussées, 6 et 8 Avenue Blaise Pascal, Cité Descartes, Champs-sur-Marne,77455 Marne-la-Vallée Cedex 2, France*
[b] *Eurotunnel Group, BP no. 69, 62904 Coquelles Cedex, France*

Abstract

In this study, a novel model for a periodically supported beam subjected to moving loads was developed using a periodicity condition on reaction forces. This condition, together with Fourier transforms and Dirac combs properties, forms a relation between the beam displacement and support reaction forces. This relation explains the force distribution to the supports, and holds for any type of support and foundation behaviors. Based on this relation, a system equivalence for a periodically supported beam is presented in this paper. An application to nonballasted viscoelastic supports is presented as an example and the results clearly match the existing model. Next, an approximation of real-time responses was developed for the moving loads as periodical series. The comparison shows that this approximation can be used for a limited number of loads if the distances between loads are sufficiently large. The system equivalence for a periodically supported beam is efficient for supports with linear behavior, and could be developed for other behaviors.

Keywords: Force distribution, Periodically supported beam, Dirac comb, Fourier transform, Nonballasted railway.

*Corresponding author
Email address: tien.hoang@enpc.fr (T. Hoang)

1. Introduction

Support systems for rails have been developed throughout the history of the railway industry. This system was initially developed with simple wood blocks, and nowadays is more complexly designed using different components and materials, and can be used without a ballast layer (so-called nonballasted railway). There is no analytical model for such a system; however, a model of a ballasted track with discrete supports is probably applicable. This is also applied to models of infinite periodically supported beams through various techniques [1–9]. Based on the wave propagation on periodical structures and Fourier series techniques, Mead [1, 2] developed a model with elastic supports and harmonic loads, while Sheng et al. [6, 7] developed one with loads from wheel–rail interactions. A periodicity condition was used by Metrikine et al. [3, 4] and Belotserkovskiy [5] to solve the system with moving concentrated forces. Nordborg [8, 9] applied the Fourier transform method and Floquet's theorem to obtain the Green's function in his model. This Green's function formulation is also used by Foda et al. [10] to calculate the response of a beam structure subjected to a moving mass.

In all these studies, the response of the beam and its supports are investigated in a complete dynamic system. To analyze the interaction between the support system and foundation, Metrikine et al. [3, 4] showed that an elastic half-space can be replaced by an equivalent stiffness. This approach suggests a new viewpoint at the interaction of the beam with its supports when separating these two components. In fact, the beam redistributes the moving forces to its supports; there are no model concerns about the mechanism of this redistribution. With this aim, a model of periodically supported beams is developed by using another version of the periodicity condition for the steady-state included in [3–5]. Further, this condition has always been presented as a boundary condition for beam displacement. In this study, this condition is introduced by considering the periodicity of the support reaction forces. Next, by using Fourier transforms and the Dirac comp properties, the periodicity condition shows a general rela-

tion between the reaction forces and beam displacements. This relation holds true for periodically supported beams with any type of support behavior (linear or nonlinear). Based on this property, a system equivalence with a stiffness and preforce for a periodically supported beam is introduced, and presents the force redistribution from the beam to its supports. This new equivalence is independent of the constitutive law of supports; thus, we can compute the response of the beam and its supports separately.

Next, an application of the system equivalence to nonballasted supports with viscoelastic behavior is presented as an example, and the results match the results given by Belotserkovskiy[5]. In addition, an approximation of real time response is developed for a periodical series of moving loads. A comparison shows that the approximation can be used when the distance between loads is sufficiently large. This model gives a general viewpoint on the interaction between the beam and its support, even if the support behavior is unknown.

2. System equivalence of a periodically supported beam

Consider a periodically supported beam, with the same constitutive law for all its supports periodically separated by a length l, as shown in Figure 1. The beam is subjected to moving forces Q_j ($1 \leq j \leq K$, K is the number of moving forces) characterized by the distance D_j to the first moving force.

Let $R_n(t)$ be the reaction force of a support at the coordinate $x = nl$ (with $n \in \mathbb{Z}$). By considering that these reaction forces are concentrated, we can locate them by utilizing Dirac functions. Therefore, the total force applied on the beam is given by

$$F(x,t) = \sum_{n=-\infty}^{\infty} R_n(t)\delta(x - nl) - \sum_{j=1}^{K} Q_j \delta(x + D_j - vt) \tag{1}$$

When using an Euler–Bernoulli homogeneous beam, the vertical displacement $w_r(x,t)$ of the beam under the total force $F(x,t)$ is solved by the following dynamic equation:

$$EI\frac{\partial^4 w_r(x,t)}{\partial x^4} + \rho S\frac{\partial^2 w_r(x,t)}{\partial t^2} - F(x,t) = 0 \tag{2}$$

where ρ is the density, E is the Young's modulus, and S and I are the section and longitudinal inertia of the beam.

Equations (1) and (2), with initial conditions, establish a relation between the beam displacement $w_r(x,t)$ and reaction forces $R_n(t)$. This relation cannot be calculated analytically because of the infinite number of unknowns. However, we could determine the periodical responses of this linear differential equation if a periodicity condition on the reaction forces is satisfied when the system is stationary (see Floquets theorem [11]). In the steady-state, all supports play the same role and their responses are supposedly equivalent and unchanged in the reference system of the moving forces. Particularly, the reaction forces of all supports are described using the same function but with a delay equal to the time for a moving load to move from one support to another. In other words, the reaction force repeats when a moving force passes from one support to another. That is, $R_n(t) = R(t - \frac{nl}{v})$ and $\hat{R}_n(\omega) = \hat{R}(\omega)e^{-i\omega\frac{nl}{v}}$, where $R(t)$ is the reaction force of the support at $x = 0$, and $\hat{R}(\omega)$ its Fourier transform.

The total force (1) in steady-state becomes

$$F(x,t) = \sum_{n=-\infty}^{\infty} R\left(t - \frac{x}{v}\right)\delta(x - nl) - \sum_{j=1}^{K} Q_j\delta(x + D_j - vt) \tag{3}$$

By substituting the last expression into equation (2), we obtain a dynamic equation of the beam in steady-state.

$$EI\frac{\partial^4 w_r(x,t)}{\partial x^4} + \rho S\frac{\partial^2 w_r(x,t)}{\partial t^2} + \sum_{j=1}^{K} Q_j\delta(x + D_j - vt) - \sum_{n=-\infty}^{\infty} R\left(t - \frac{x}{v}\right)\delta(x - nl) = 0 \tag{4}$$

Equation (4) has two unknowns: $R(t)$ and $w_r(x,t)$. We transformed this equation by performing a double Fourier transform: one temporal and one spatial. By using the properties of Dirac delta function [12], the Fourier transform of equation (4) with respect to time t gives

$$EI\frac{\partial^4 \hat{w}_r(x,\omega)}{\partial x^4} - \rho S\omega^2\hat{w}_r(x,\omega) + \sum_{j=1}^{K}\frac{Q_j}{v}\mathrm{e}^{-\mathrm{i}\frac{\omega}{v}(x+D_j)} - \hat{R}(\omega)\sum_{n=-\infty}^{\infty}\mathrm{e}^{-\mathrm{i}\frac{\omega}{v}x}\delta(x - nl) = 0 \tag{5}$$

where $\hat{w}_r(x,\omega)$ and $\hat{R}(\omega)$ are the Fourier transforms of $w_r(x,t)$ and $R(t)$, respectively. Furthermore, by applying the spatial Fourier transform of the last

result with respect to x gives

$$(EI\lambda^4 - \rho S\omega^2)\Pi(\lambda,\omega) + 2\pi\delta\left(\lambda + \frac{\omega}{v}\right)\sum_{j=1}^{K}\frac{Q_j}{v}\mathrm{e}^{-\mathrm{i}\frac{\omega}{v}D_j} - \hat{R}(\omega)\sum_{n=-\infty}^{\infty}\mathrm{e}^{-\mathrm{i}(\lambda+\frac{\omega}{v})nl} = 0 \quad (6)$$

where $\Pi(\lambda,\omega)$ is the Fourier transform of $\hat{w}_r(x,\omega)$ with respect to x. The last term in equation (6) is a Dirac comb [12], which has the following property:

$$\sum_{n=-\infty}^{\infty}\mathrm{e}^{-\mathrm{i}\left(\lambda+\frac{\omega}{v}\right)nl} = \frac{2\pi}{l}\sum_{n=-\infty}^{\infty}\delta\left(\lambda + \frac{\omega}{v} + \frac{2\pi n}{l}\right) \quad (7)$$

Then, $\Pi(\lambda,\omega)$ can be obtained from equation (6):

$$\Pi(\lambda,\omega) = \frac{2\pi\hat{R}(\omega)}{lEI(\lambda^4-\lambda_e^4)}\sum_{n=-\infty}^{\infty}\delta\left(\lambda + \frac{\omega}{v} + \frac{2\pi n}{l}\right) - \frac{2\pi\delta\left(\lambda+\frac{\omega}{v}\right)}{vEI(\lambda^4-\lambda_e^4)}\sum_{j=1}^{K}Q_j\mathrm{e}^{-\mathrm{i}\frac{\omega}{v}D_j} \quad (8)$$

where $\lambda_e = \sqrt[4]{\frac{\rho S\omega^2}{EI}}$ (subscript e for the Euler–Bernoulli beam).

Next, the expression of $\hat{w}_r(x,\omega)$ is deduced by performing the inverse Fourier transform of $\Pi(\lambda,\omega)$.

$$\hat{w}_r(x,\omega) = \frac{\hat{R}(\omega)}{lEI}\sum_{n=-\infty}^{\infty}\frac{\mathrm{e}^{-\mathrm{i}\left(\frac{\omega}{v}+\frac{2\pi n}{l}\right)x}}{\left(\frac{\omega}{v}+\frac{2\pi n}{l}\right)^4 - \lambda_e^4} - \sum_{j=1}^{K}\frac{Q_j\mathrm{e}^{-\mathrm{i}\frac{\omega}{v}(x+D_j)}}{vEI\left[\left(\frac{\omega}{v}\right)^4-\lambda_e^4\right]} \quad (9)$$

For instance, the vertical displacement of the beam at $x = 0$ is as follows.

$$\hat{w}_r(0,\omega) = \frac{\hat{R}(\omega)}{lEI}\sum_{n=-\infty}^{\infty}\frac{1}{\left(\frac{\omega}{v}+\frac{2\pi n}{l}\right)^4 - \lambda_e^4} - \sum_{j=1}^{K}\frac{Q_j\mathrm{e}^{-\mathrm{i}\omega\frac{D_j}{v}}}{vEI\left[\left(\frac{\omega}{v}\right)^4-\lambda_e^4\right]} \quad (10)$$

By introducing a function $\eta_e(\omega)$,

$$\eta_e(\omega) = \frac{1}{lEI}\sum_{n=-\infty}^{\infty}\frac{1}{\left(\frac{\omega}{v}+\frac{2\pi n}{l}\right)^4 - \lambda_e^4} \quad (11)$$

This can also be written as follows (see Appendix A1):

$$\eta_e(\omega) = \frac{1}{4\lambda_e^3 EI}\left[\frac{\sin l\lambda_e}{\cos l\lambda_e - \cos\frac{\omega l}{v}} - \frac{\sinh l\lambda_e}{\cosh l\lambda_e - \cos\frac{\omega l}{v}}\right] \quad (12)$$

Equation (10) becomes

$$\hat{w}_r(0,\omega) = \hat{R}(\omega)\eta_e(\omega) - \sum_{j=1}^{K}\frac{Q_j\mathrm{e}^{-\mathrm{i}\omega\frac{D_j}{v}}}{vEI\left[\left(\frac{\omega}{v}\right)^4-\lambda_e^4\right]} \quad (13)$$

This equation can also be written in the following form:

$$\hat{R}(\omega) = \mathcal{K}_e \hat{w}_r(0,\omega) + \mathcal{Q}_e \tag{14}$$

where $\mathcal{K}_e = \eta_e^{-1}(\omega)$ and $\mathcal{Q}_e$ is defined by

$$\mathcal{Q}_e = \frac{\sum_{j=1}^{K} Q_j \mathrm{e}^{-\mathrm{i}\omega\frac{D_j}{v}}}{vEI\eta_e(\omega)\left[\left(\frac{\omega}{v}\right)^4 - \lambda_e^4\right]} \tag{15}$$

In fact, equation (14) is a relationship between the vertical displacement of the rail and the reaction force at $x = 0$. From equations (9) and (10), we obtain the displacement at other supports as follows.

$$\hat{w}(nl,\omega) = \hat{w}(0,\omega)\mathrm{e}^{-\mathrm{i}\omega\frac{nl}{v}} \tag{16}$$

This equation shows that the displacement of the beam at $x = nl$ is also repeated as the periodic condition for the reaction forces. Therefore, if we multiply equation (14) by $\mathrm{e}^{-\mathrm{i}\omega\frac{nl}{v}}$, we obtain

$$\hat{R}_n(\omega) = \mathcal{K}_e \hat{w}_r(nl,\omega) + \mathcal{Q}_e \mathrm{e}^{-\mathrm{i}\omega\frac{nl}{v}} \tag{17}$$

The aforementioned equation is exactly equivalent to equation (14) for the support at $x = nl$, when $\mathcal{Q}_e$ is calculated using a delay $t = \frac{nl}{v}$, which is equal to the time for the force to move from the support at $x = 0$ to the support at $x = nl$. Hence, we can represent any periodically supported beam by using a spring of stiffness $\mathcal{K}_e$ and preforce $\mathcal{Q}_e$, as shown in Figure 2. We note that the stiffness has no imaginary part. The beam distributes the force to each support according to their distance, that is, the further away the support is, the lower the force applied is. In other words, the force increases and decreases progressively when the force moves toward and away from the support. This force distribution process is the same as a preforced spring application on the support. Therefore, we obtain the system equivalence for a periodically supported beam with two parameters (preforce $\mathcal{Q}_e$ and stiffness $\mathcal{K}_e$).

Remark

By combining equations (15) and (9), we obtain

$$\hat{w}_r(x,\omega) = \hat{R}(\omega)\eta(x,\omega) - \mathcal{Q}_e\eta_e(\omega)\mathrm{e}^{-\mathrm{i}\frac{\omega}{v}x} \tag{18}$$

Table 1: Parameters of a periodically supported beam

Section mass (ρS)	kg/m	60
Section stiffness (EI)	MNm^2	6.3
Sleeper length (l)	m	0.6

where $\eta(x,\omega)$ is defined as

$$\eta(x,\omega) = \frac{1}{lEI} \sum_{n=-\infty}^{\infty} \frac{\mathrm{e}^{-\mathrm{i}\left(\frac{\omega}{v}+\frac{2\pi n}{l}\right)x}}{\left(\frac{\omega}{v}+\frac{2\pi n}{l}\right)^4 - \lambda_e^4} \tag{19}$$

This function can be reduced (see Appendix A1) as follows:

$$\eta(x,\omega) = \frac{1}{4\lambda_e^3 EI}\left[\frac{\sin\lambda_e(l-x) + \mathrm{e}^{-\mathrm{i}\frac{\omega l}{v}}\sin\lambda_e x}{\cos l\lambda_e - \cos\frac{\omega l}{v}} - \frac{\sinh\lambda_e(l-x) + \mathrm{e}^{-\mathrm{i}\frac{\omega l}{v}}\sinh\lambda_e x}{\cosh l\lambda_e - \cos\frac{\omega l}{v}}\right] \tag{20}$$

Equation (18) is another relation between the beam displacement and support reaction force. Moreover, this relation holds true for all types of supports and is equivalent to the dispersion relation presented in [8], when the reaction force is proportional to the displacement and the propagation coefficient is imaginary.

Example

Now, we consider a periodically supported beam by using the parameters given in Table 1. Figure 3 shows the frequency stiffness $\mathcal{K}_e$ for different speeds. The stiffness is observed to reach a maximum frequency of approximately $(0.5+n)v/l$ ($n \in \mathbb{Z}$). Frequencies nv/l correspond to the movement of a force from one support to another, and the maximum peaks explain the coupling of the beam and its supports. In addition, the equivalent stiffness can be negative at high frequencies. This phenomenon occurs due to supports being subjected to a vertical traction when the forces approach or move away, particularly at high speed. This characteristic is important because most support systems are not designed to support pulled forces.

Figure 4 shows the preforce $\mathcal{Q}_e$ for a moving force $Q = 100$kN with different speeds. It is remarkable that the preforce is important at low frequencies

only. Furthermore, a higher speed indicates a higher excited frequency. This characteristic may be useful to estimate efficient bandwidths of frequencies for analyzing properties of a foundation used in a high-speed railway design.

By combining equations (14) and (18) with the constitutive law of the support, the problem of a periodically supported beam can be solved efficiently. In the next section, we show the application of this system equivalence to supports with a linear viscoelastic behavior and the development of an approximation of real-time responses.

3. Application to supports with viscoelastic behavior

Consider a support system for a nonballasted track including an independent concrete block, two polymer pads (one under the rail and another under the block), and a rubber boot. Damping is considered for a Kelvin–Voigt viscoelastic model [13], as shown in Figure 5.

Let $w_s(t)$ denote the vertical displacement of the concrete block. This displacement is governed by the following equation:

$$M\frac{\mathrm{d}^2 w_s(t)}{\mathrm{d}t^2} + \eta_2\frac{\mathrm{d}w_s(t)}{\mathrm{d}t} + k_2 w_s(t) = -R(t) \tag{21}$$

where M is the mass of the block and η_2 and k_2 are the damping and spring coefficients of the boot with a pad under the block. The force $R(t)$ is given as

$$R(t) = -\eta_1\frac{\mathrm{d}(w_r(0,t) - w_s(t))}{\mathrm{d}t} - k_1(w_r(0,t) - w_s(t)) \tag{22}$$

where η_1 and k_1 are the damping and spring coefficients of the rail pad.

By applying the Fourier transform to the two aforementioned equations, we obtain

$$(-M\omega^2 + \mathrm{i}\eta_2\omega + k_2)\hat{w}_s(\omega) = -\hat{R}(\omega) \tag{23}$$

$$\hat{R}(\omega) = (\mathrm{i}\eta_1\omega + k_1)\left[\hat{w}_r(0,\omega) - \hat{w}_s(\omega)\right] \tag{24}$$

where $\hat{w}_s$ and $\hat{w}_r$ are the Fourier transforms of w_s and w_r, respectively. Next,

we deduce

$$\hat{R}(\omega) = -k_s \hat{w}_r(0,\omega) \tag{25}$$

$$\hat{w}_s(\omega) = \frac{k_s \hat{w}_r(0,\omega)}{-M\omega^2 + \mathrm{i}\eta_2\omega + k_2} \tag{26}$$

where k_s is the stiffness of the support system.

$$k_s = \frac{(\mathrm{i}\eta_1\omega + k_1)(-M\omega^2 + \mathrm{i}\eta_2\omega + k_2)}{-M\omega^2 + \mathrm{i}(\eta_1+\eta_2)\omega + k_1 + k_2} \tag{27}$$

Equation (25) is a linear relation between $\hat{R}(\omega)$ and $\hat{w}_r(0,\omega)$. By combining this relation and the system equivalence, we can thus determine the response of the system.

Responses in the frequency domain

The response of a support is deduced from equations (14) and (25):

$$\hat{w}_r(0,\omega) = \frac{-\mathcal{Q}_e}{k_s + \mathcal{K}_e} \tag{28}$$

$$\hat{R}(\omega) = \frac{k_s \mathcal{Q}_e}{k_s + \mathcal{K}_e} \tag{29}$$

Further, by substituting equations (28) and (29) into equation (18), the beam response is given as

$$\hat{w}_r(x,\omega) = -\mathcal{Q}_e \left[\eta_e(\omega) \mathrm{e}^{-\mathrm{i}\frac{\omega}{v}x} - \frac{k_s \eta(x,\omega)}{k_s + \mathcal{K}_e} \right] \tag{30}$$

Equation (30) is identical to the analytical result given by Belotserkovkiy [5] by considering a periodicity of the beam displacement. This result suggests the reduction of $\eta(x,\omega)$ in Appendix A1 from its Fourier series; this is not easy to calculate analytically.

Equations (29) and (30) form complete responses in the frequency domain of the beam and its support. The time responses are calculated using the inverse Fourier transform of these results.

Vertical vibration of the loading point

By applying the inverse Fourier transform of equation (30), we determine the beam displacement through the following equation:

$$\begin{aligned} w_r(x,t) &= \frac{1}{2\pi}\int_{-\infty}^{\infty} -\mathcal{Q}_e\left[\eta_e(\omega)\mathrm{e}^{-\mathrm{i}\frac{\omega}{v}x} - \frac{k_s\eta(x,\omega)}{k_s+\mathcal{K}_e}\right]\mathrm{e}^{\mathrm{i}\omega t}\mathrm{d}\omega \\ &= \frac{-1}{2\pi}\int_{-\infty}^{\infty}\frac{\mathcal{Q}_e\mathrm{e}^{-\mathrm{i}\frac{\omega}{v}(x-vt)}\mathrm{d}\omega}{k_s+\mathcal{K}_e} - \frac{1}{2\pi}\int_{-\infty}^{\infty}\left[\eta_e(\omega)\mathrm{e}^{-\mathrm{i}\frac{\omega}{v}x} - \eta(x,\omega)\right]\frac{k_s\mathcal{Q}_e\mathrm{e}^{\mathrm{i}\omega t}\mathrm{d}\omega}{k_s+\mathcal{K}_e} \end{aligned}$$

Here, we used the following equation: $\mathcal{K}_e = \eta_e^{-1}(\omega)$. The loading point has a vertical displacement, which is the same as the beam displacement at coordinate $x = vt$. Hence, we can deduce this displacement denoted by $w_w(t)$ by substituting vt for x in the last expression.

$$w_w(t) = \frac{-1}{2\pi}\int_{-\infty}^{\infty}\frac{\mathcal{Q}_e\mathrm{d}\omega}{k_s+\mathcal{K}_e} - \frac{1}{2\pi}\int_{-\infty}^{\infty}\frac{k_s\mathcal{Q}_e}{k_s+\mathcal{K}_e}\left[\eta_e(\omega) - \eta(vt,\omega)\mathrm{e}^{\mathrm{i}\omega t}\right]\mathrm{d}\omega \qquad (31)$$

By applying the inverse Fourier transform of equation (28) with $t = 0$, we obtain

$$w_r(0,0) = \frac{1}{2\pi}\int_{-\infty}^{\infty}\frac{-\mathcal{Q}_e\mathrm{d}\omega}{k_s+\mathcal{K}_e} \qquad (32)$$

Next, by substituting this result into equation (31), we obtain

$$w_w(t) = w_r(0,0) - \frac{1}{2\pi}\int_{-\infty}^{\infty}\frac{k_s\mathcal{Q}_e}{k_s+\mathcal{K}_e}\left[\eta_e(\omega) - \eta(vt,\omega)\mathrm{e}^{\mathrm{i}\omega t}\right]\mathrm{d}\omega \qquad (33)$$

Thus, the loading point has a vertical motion around the position $w_r(0,0)$. Because $\eta(vt,\omega)$ is periodical with respect to t, the vertical motion is periodical in terms of frequency $f = v/l$ described by the second term of equation (33). The amplitude A_0 of this motion can be obtained at the midpoint of two supports corresponding to $t = \frac{l}{2v}$.

$$A_0 = \frac{1}{2\pi}\int_{-\infty}^{\infty}\frac{k_s\tilde{\eta}_e}{k_s+\mathcal{K}_e}\mathcal{Q}_e\mathrm{d}\omega \qquad (34)$$

where $\tilde{\eta}_e(\omega)$ is defined by

$$\tilde{\eta}_e(\omega) = \left[\eta_e(\omega) - \eta(vt,\omega)\mathrm{e}^{\mathrm{i}\omega t}\right]_{t=\frac{l}{2v}} \qquad (35)$$

This can also be written (see Appendix A2) in the following form:

$$\tilde{\eta}_e(\omega) = \frac{1}{8\lambda_e^3 EI}\left[\frac{\sin\frac{l\lambda_e}{2}}{\cos\frac{l\lambda_e}{2}-\cos\frac{l\omega}{2v}} - \frac{\sinh\frac{l\lambda_e}{2}}{\cosh\frac{l\lambda_e}{2}-\cos\frac{l\omega}{2v}}\right] \tag{36}$$

Equation (33) with amplitude (34) describes the vertical movement of the loading point. This can be used for the contact wheel–rail analysis mentioned in [9].

Approximation of time responses

Consider a periodical series of moving loads. These can be used to represent the load charges of a train with many wagons of equal masses (e.g., a passenger train fully charged, as shown in Figure 6). Such loads can be estimated as a series of identical charges ($Q_j = Q$) characterized by distances to a reference charge given by

$$D_j = \begin{cases} jH & \text{if j is even} \\ jH + D & \text{if j is odd} \end{cases}$$

where H is the length of a wagon and D is the distance between two wheels of a boogie. By using the Dirac comb property, we have

$$\sum_{j=-\infty}^{\infty} Q_j \mathrm{e}^{-\mathrm{i}\omega\frac{D_j}{v}} = \frac{2\pi v Q}{H}\left(1+\mathrm{e}^{-\mathrm{i}\omega\frac{D}{v}}\right)\sum_{j=-\infty}^{\infty}\delta\left(\omega+\frac{2\pi v}{H}j\right)$$

By combining the aforementioned equation with equation (15), we have

$$\mathcal{Q}_e(\omega) = \frac{2\pi Q\left(1+\mathrm{e}^{-\mathrm{i}\omega\frac{D}{v}}\right)}{HEI\eta_e\left[\left(\frac{\omega}{v}\right)^4-\lambda_e^4\right]}\sum_{j=-\infty}^{\infty}\delta\left(\omega+\frac{2\pi v}{H}j\right) \tag{37}$$

By substituting this equation into equation (28) and developing the inverse Fourier transform,

$$\begin{aligned}\hat{w}_r(0,t) &= \frac{-Q}{2\pi HEI}\int_{-\infty}^{\infty}\frac{2\pi\left(1+\mathrm{e}^{-\mathrm{i}\omega\frac{D}{v}}\right)\mathrm{e}^{\mathrm{i}\omega t}\mathrm{d}\omega}{(k_s\eta_e+1)\left[\left(\frac{\omega}{v}\right)^4-\lambda_e^4\right]}\sum_{j=-\infty}^{\infty}\delta\left(\omega+\frac{2\pi v}{H}j\right) \\ &= -\frac{Q}{HEI}\sum_{j=-\infty}^{\infty}\left[\frac{\left(1+\mathrm{e}^{-\mathrm{i}\omega\frac{D}{v}}\right)\mathrm{e}^{\mathrm{i}\omega t}}{(1+k_s\eta_e)\left(\left(\frac{\omega}{v}\right)^4-\lambda_e^4\right)}\right]_{\omega=-\omega_j}\end{aligned} \tag{38}$$

where $\omega_j = 2\pi j \frac{v}{H}$.

Similarly, the following analytic solution can be determined through equation (29)for the response of the railway track:

$$R(t) = \frac{Q}{HEI} \sum_{j=-\infty}^{\infty} \left[\frac{k_s \left(1 + \mathrm{e}^{-\mathrm{i}\omega \frac{D}{v}}\right) \mathrm{e}^{\mathrm{i}\omega t}}{(1 + k_s \eta_e) \left(\left(\frac{\omega}{v}\right)^4 - \lambda_e^4 \right)} \right]_{\omega = -\omega_j} \tag{39}$$

Expressions (38) and (39) are Fourier series of frequency $f_0 = \frac{v}{H}$. Thus, the responses of a periodically supported beam subjected to a periodical series of moving loads comprise vibrations of the same frequency f_0.

Example

Here, we calculate the responses by using different formulas of the model and compare the results. Consider a periodically supported beam with parameters, as shown in Tables 1 and 2. By using the inverse Fourier transform of equation (29), we compute the support reaction force under a couple of moving charges $Q = 100$ kN with a distance $D = 3$ m between them. Then, we can calculate a periodical series of charges $Q = 100$ kN with $H = 18$ m and $D = 3$ m (see Figure 6) by using equation (39). Finally, the beam displacement is calculated by using equation (30).

Figure 7 shows that the time responses obtained through the inverse Fourier transform of equation (29) and equation (39) give accurate results in one period H/v. Therefore, the approximation of time response is proposed for moving loads when the distances between loads are sufficiently large. The calculation obtained using this analytical expression is almost instantaneous.

Figure 8 shows the displacement of a beam of length H for three positions of the reference charge: on the top of the support ($x = 0$), at the middle of two supports ($x = l/2$), and on the top of the next support ($x = l$). The results show that the curves almost have a similar form with a translation along the direction of movement. However, equation (34) shows that the maximum displacement at the middle position ($x = l/2$) is greater than at the other two positions ($A_0 = 2.7\mu$ m).

Table 2: Parameters of viscoelastic support

Block mass (M)	kg	100
Damping factor of rail pad (η_1)	$MNsm^{-1}$	1.97
Stiffness of rail pad (k_1)	MNm^{-1}	192
Damping coeff. under support (η_2)	$MNsm^{-1}$	0.17
Stiffness under support (k_2)	MNm^{-1}	26.4

The dynamic responses of a railway track using the support system shown in Figure 5 were measured at the Channel tunnel in 2005. Displacement sensors were positioned at four corners of the concrete block and at the rail foot corresponding to the four corners of the rail pad (see Figure 9). In addition, strain gauges were placed on the neutral axis of the rail to measure the reaction force via the shear stress of two cross-sections of the rail. The measurements were recorded during a normal passenger train traffic. The displacement of the block and rail were calculated as the average of the four displacement sensor signals in the four corners. The reaction force is the signal of the strain gauges after calibration with a static measurement. As most of the train's wagons are of the same length, the result signals were almost periodic. Therefore, the final results were computed as the average of all signal periods. An advantage of these measurements is that the railway track was being used under real conditions. However, the properties of the support components located in the railway track were not measured. Here, we computed the responses by using the model with parameters of a new support system before its installation in the railway track, as shown in Table 2. These stiffness parameters of the pads were measured through compression at speed 50 kN/mm and their damping coefficients were measured at a frequency of 5 Hz.

Figures 10 and 11 show the reaction force of a support and the vertical displacement of the rail at the support position through the measurement and model, respectively. The responses of the force are observed to be more accurate than the displacement. In fact, the displacement was not measured at the

neutral line of the rail as it could have been influenced by local deformations.

4. Conclusion

In this study, the system equivalence of a periodically supported beam was developed and applied to a nonballasted railway track. This system equivalence explains how the beam redistributes the forces to its supports, as well as the efficient bandwidths of excited frequencies, even if the support and foundation behaviors are unknown. Therefore, this model has some advantages compared to existing models because the force distribution can be useful for studying the independent behaviors of the support and foundation. Moreover, the analytic approximations for linear supports were established and can be used to calculate the real-time responses if the distances between loads are sufficiently large.

Appendix

A1. Calculation of expression $\eta(x,\omega)$

From equation (19), we have

$$\begin{aligned}\eta(x,\omega) &= \frac{1}{lEI}\sum_{n=-\infty}^{\infty}\frac{\mathrm{e}^{-\mathrm{i}\left(\frac{\omega}{v}+\frac{2\pi n}{l}\right)x}}{\left(\frac{\omega}{v}+\frac{2\pi n}{l}\right)^4-\lambda_e^4}\\ &= \frac{l\mathrm{e}^{-\mathrm{i}\frac{\omega}{v}x}}{2\lambda_e^2EI}\left[\sum_{n=-\infty}^{\infty}\frac{\mathrm{e}^{-\mathrm{i}2\pi n\frac{x}{l}}}{\left(\frac{\omega l}{v}+2\pi n\right)^2-(l\lambda_e)^2}-\sum_{n=-\infty}^{\infty}\frac{\mathrm{e}^{-\mathrm{i}2\pi n\frac{x}{l}}}{\left(\frac{\omega l}{v}+2\pi n\right)^2+(l\lambda_e)^2}\right]\end{aligned}$$

We show that each term of this expression can be deduced as follows:

$$\sum_{n=-\infty}^{\infty}\frac{\mathrm{e}^{-\mathrm{i}2\pi n\frac{x}{l}}}{\left(\frac{\omega l}{v}+2\pi n\right)^2-(l\lambda_e)^2} = \frac{\mathrm{e}^{\mathrm{i}\frac{\omega}{v}x}}{2l\lambda_e}\frac{\sin\lambda_e(l-x)+\mathrm{e}^{-\mathrm{i}\frac{\omega l}{v}}\sin\lambda_e x}{\cos l\lambda_e-\cos\frac{\omega l}{v}} \quad (40)$$

$$\sum_{n=-\infty}^{\infty}\frac{\mathrm{e}^{-\mathrm{i}2\pi n\frac{x}{l}}}{\left(\frac{\omega l}{v}+2\pi n\right)^2+(l\lambda_e)^2} = \frac{\mathrm{e}^{\mathrm{i}\frac{\omega}{v}x}}{2l\lambda_e}\frac{\sinh\lambda_e(l-x)+\mathrm{e}^{-\mathrm{i}\frac{\omega l}{v}}\sinh\lambda_e x}{\cosh l\lambda_e-\cos\frac{\omega l}{v}} \quad (41)$$

and therefore we obtain the result:

$$\eta(x,\omega)=\frac{1}{4\lambda_e^3EI}\left[\frac{\sin\lambda_e(l-x)+\mathrm{e}^{-\mathrm{i}\frac{\omega l}{v}}\sin\lambda_e x}{\cos l\lambda_e-\cos\frac{\omega l}{v}}-\frac{\sinh\lambda_e(l-x)+\mathrm{e}^{-\mathrm{i}\frac{\omega l}{v}}\sinh\lambda_e x}{\cosh l\lambda_e-\cos\frac{\omega l}{v}}\right] \quad (42)$$

In fact, the right-hand sides of equations (40) and (41) represent expressions of Fourier series with respect to the variable x. Therefore, it is sufficient to

demonstrate that the Fourier series coefficients of the functions on the left-hand sides correspond to coefficients of the series on the right-hand sides.

Let $f(x)$ be the function on the left-hand side of equation (40). This function is continuous, derivable, and periodic with the period l. Therefore, its Fourier series development converges. By definition, the Fourier series coefficient of $f(x)$ is computed as

$$\begin{aligned} c_{-n} &= \frac{1}{l}\int_0^l f(x)\mathrm{e}^{\mathrm{i}2\pi n\frac{x}{l}}\mathrm{d}x \\ &= \frac{1}{l}\int_0^l \frac{\mathrm{e}^{\mathrm{i}\frac{\omega}{v}x}}{2l\lambda_e}\frac{\sin\lambda_e(l-x)+\mathrm{e}^{-\mathrm{i}\frac{\omega l}{v}}\sin\lambda_e x}{\cos l\lambda_e-\cos\frac{\omega l}{v}}\mathrm{e}^{\mathrm{i}2\pi n\frac{x}{l}}\mathrm{d}x \\ &= \int_0^l \frac{\left[\sin\lambda_e(l-x)+\mathrm{e}^{-\mathrm{i}\frac{\omega l}{v}}\sin\lambda_e x\right]\mathrm{e}^{\mathrm{i}\left(\frac{\omega l}{v}+2\pi n\right)x}\mathrm{d}x}{2l^2\lambda_e\left(\cos l\lambda_e-\cos\frac{\omega l}{v}\right)} \end{aligned}$$

The aforementioned expression is an integral of a trigonometric function, which can easily be calculated to obtain the following result:

$$c_{-n} = \frac{1}{\left(\frac{\omega l}{v}+2\pi n\right)^2-(l\lambda_e)^2} \tag{43}$$

Thus, the right-hand side of equation (40) represents the Fourier series of $f(x)$, and equation (40) is proved. Similarly, we can prove equation (41); therefore, equation (42) is proved.

Particularly, when $x=0$ we have

$$\begin{aligned} \eta(0,\omega) &= \frac{1}{lEI}\sum_{n=-\infty}^{\infty}\frac{1}{\left(\frac{\omega}{v}+\frac{2\pi n}{l}\right)^4-\lambda_e^4} \\ &= \frac{1}{4\lambda_e^3 EI}\left[\frac{\sin l\lambda_e}{\cos l\lambda_e-\cos\frac{\omega l}{v}}-\frac{\sinh l\lambda_e}{\cosh l\lambda_e-\cos\frac{\omega l}{v}}\right] \end{aligned}$$

These two expressions are exactly the definition and the reduced formulae of $\eta_e(\omega)$ in equations (11) and (12).

A2. Calculation of expression $\tilde{\eta}_e(\omega)$

By substituting equations (11) and (19) (with $x = l/2$) into equation (35), we have

$$\begin{aligned}\tilde{\eta}_e(\omega) &= \frac{1}{lEI}\sum_{n=-\infty}^{\infty}\frac{1-\mathrm{e}^{-\mathrm{i}\pi n}}{\left(\frac{\omega}{v}+\frac{2\pi n}{l}\right)^4-\lambda_e^4} \\ &= \frac{1}{2}\left[\frac{1}{(l/2)EI}\sum_{p=-\infty}^{\infty}\frac{1}{\left(\frac{\omega}{v}+\frac{2\pi p}{l/2}\right)^4-\lambda_e^4}\right]\end{aligned}$$

The formula in brackets is exactly the formula of $\eta_e(\omega)$ in equation (11) but with the parameter $l/2$ instead of l. Hence, we deduced the result in equation (36).

List of Figures

[1] D. J. Mead, Free wave propagation in periodically supported, infinite beams, Journal of Sound and Vibration 11 (2) (1970) 181–197.

[2] D. J. Mead, Wave propagation in continuous periodic structures: research contributions from southampton, Journal of Sound and Vibration 190 (3) (1996) 495–524.

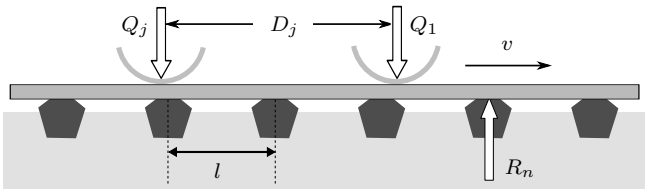

Figure 1: Periodically supported beam subjected to moving loads

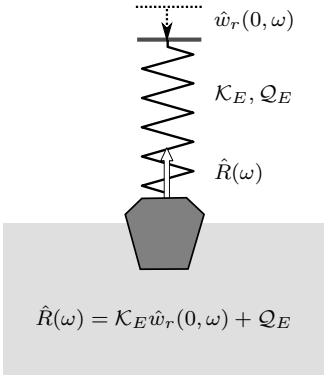

Figure 2: System equivalence of periodically supported beams

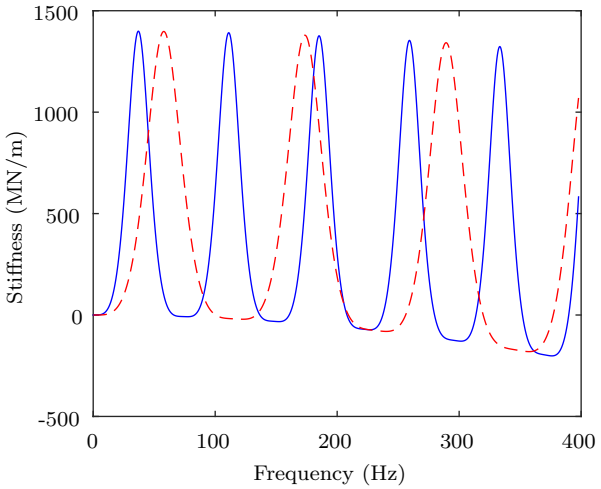

Figure 3: Equivalent stiffness $\mathcal{K}_e$ with $v = 160$km/h (continuous blue line) and $v = 250$km/h (dashed red line)

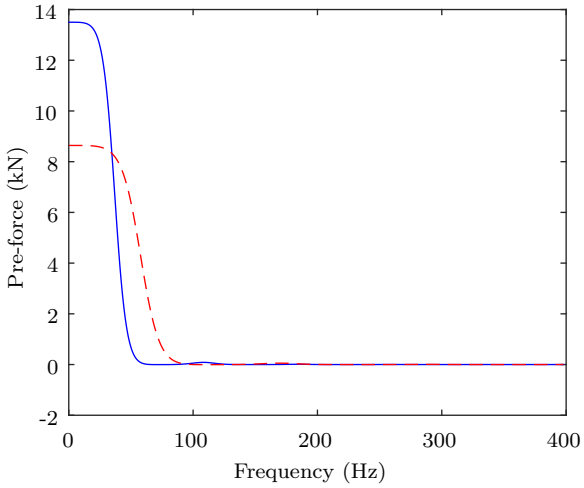

Figure 4: Equivalent preforce $\mathcal{Q}_e$ for a single moving load $Q = 100$kN with $v = 160$km/h (continuous blue line) and $v = 250$km/h (dashed red line)

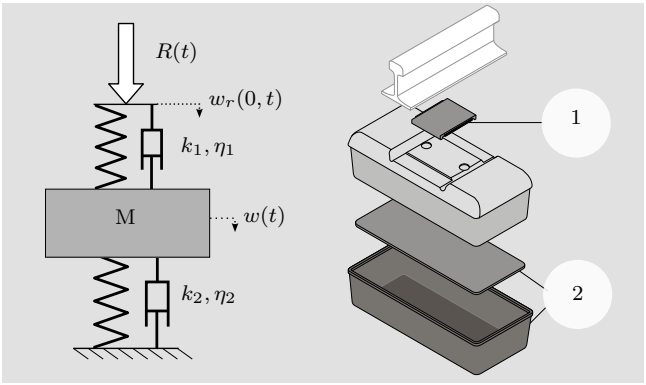

Figure 5: Model of a nonballasted railway support with rail pad (1), block pad and boot (2)

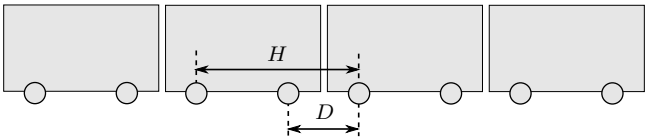

Figure 6: Charges of a train as a periodical series of moving loads

[3] A. V. Metrikine, K. Popp, Vibration of a periodically supported beam on an elastic half-space, European Journal of Mechanics A/Solid 18 (1999)

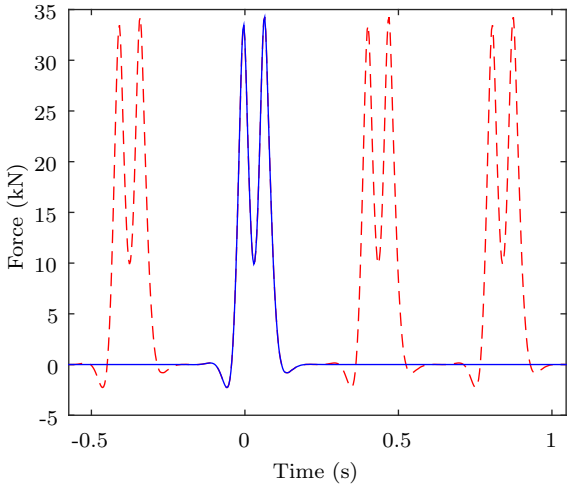

Figure 7: Support reaction forces to a couple of moving loads (continuous blue line) and to a periodical series of moving loads (dashed red line)

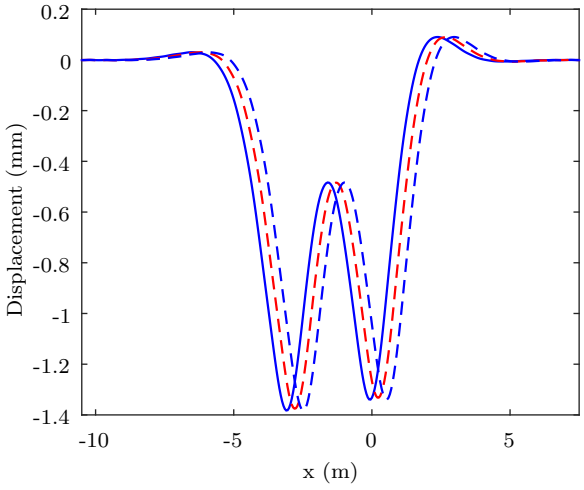

Figure 8: Beam displacement for 3 positions of the moving loads: at the support position (continuous blue line), at the center of two supports (dash red line) and at the next support position (dashed blue line)

679–701.

[4] A. V. Vostroukhov, A. Metrikine, Periodically supported beam on a visco-

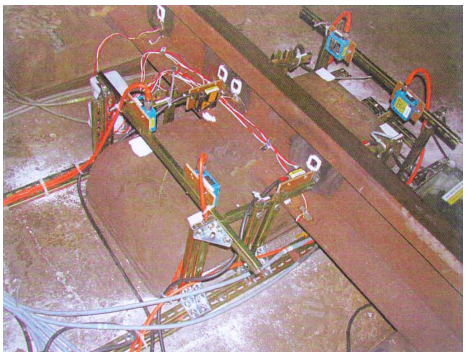

Figure 9: Measurement schema in situ

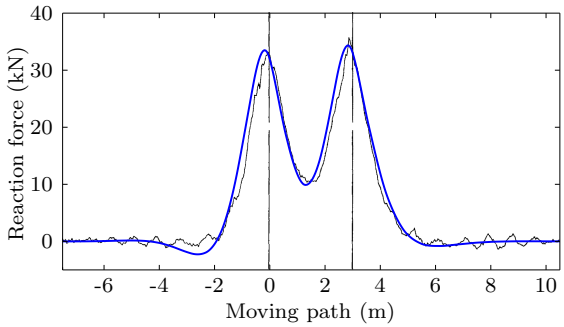

Figure 10: Reaction force by the measurements in situ (black line) and analytic model (blue line)

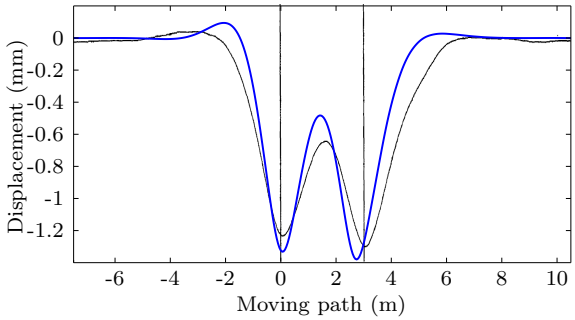

Figure 11: Rail displacement at the support position by the measurements in situ (black line) and analytic model (blue line)

elastic layer as a model for dynamic analysis of a high-speed railway track, International Journal of Solids and Structures 40 (2003) 5723–5752.

[5] P. M. Belotserkovskiy, On the oscillation of infinite periodic beams subjected to a moving concentrated force, Journal of Sound and Vibration 193 (3) (1996) 705–712.

[6] X. Sheng, C. Jones, D. Thompson, Response of infinite periodic structure to moving or stationary harmonic loads, Journal of Sound and Vibration 282 (2005) 125–149.

[7] X. Sheng, M. Li, C. Jones, D. Thompson, Using the Fourier-series approach to study interactions between moving wheels and a periodically supported rail, Journal of Sound and Vibration 303 (2007) 873–894.

[8] A. Nordborg, Vertical rail vibrations: Pointforce excitation, Acustica 84 (1998) 280–288.

[9] A. Nordborg, Vertical rail vibrations: Parametric excitation, Acustica 84 (1998) 289–300.

[10] M. A. Foda, Z. Abduljabbar, A dynamic Green function formulation for the response of a beam structure to a moving mass, Journal of Sound and Vibration 210 (2) (1998) 295–306.

[11] W. Walter, Ordinary differential equations, Springer, 1998.

[12] R. Bracewell, The Fourier Transform and Its Applications, McGraw-Hill Higher Education, 2000.

[13] R. M. Christensen, Theory of Viscoelasticity, 2nd Edition, Dover Plublication, 2003.